



Green roofs and green walls layouts for improved urban air quality by mitigating particulate matter



Margareth Viecco ^{a,b,c}, Héctor Jorquera ^{c,d}, Ashish Sharma ^e, Waldo Bustamante ^{c,f}, Harindra J. S. Fernando ^g, Sergio Vera ^{a,c,*}

^a Department of Construction Engineering and Management, Pontificia Universidad Católica de Chile, Santiago, 7820436, Chile

^b Faculty of Civil Engineering, Universidad Pontificia Bolivariana, Bucaramanga, 681007, Colombia

^c Center for Sustainable Urban Development (CEDEUS), Pontificia Universidad Católica de Chile, Santiago, 7520246, Chile

^d Department of Chemical Engineering and Bioprocesses, Pontificia Universidad Católica de Chile, Santiago, 7820436, Chile

^e Climate and Atmospheric Science Section, Illinois State Water Survey, Prairie Research Institute, and the Department of Atmospheric Sciences, University of Illinois at Urbana-Champaign, Champaign, IL, 61820, USA

^f School of Architecture, Pontificia Universidad Católica de Chile, Santiago, 7520245, Chile

^g Department of Civil & Environmental Engineering and Earth Sciences (CEES), University of Notre Dame, 156 Fitzpatrick Hall, Notre Dame, IN, 46556, USA

ARTICLE INFO

Keywords:

Urban air pollution modeling
Green roofs
Green walls
PM_{2.5} capture
PM_{2.5} concentration
Urban morphology

ABSTRACT

Urban air quality has been a long-standing problem in most cities worldwide. Many strategies have been proposed to solve it, including green infrastructures such as green roofs (GRs) and green walls (GWS) that provide multiple environmental benefits. Many studies have focused on GRs and GWS strategies to mitigate urban air pollution. However, to the best of authors' knowledge, these studies have not dealt with different urban morphologies, specifically the impact of building heights and coverage ratios of GRs and GWS on mitigating air pollution. Therefore, the potential of GRs and GWS to alleviate air pollution has not been fully exploited. This paper aims to investigate different GRs and GWS layouts and evaluate their efficacy for capturing particulate matter (PM_{2.5}) in an urban neighborhood of Santiago, Chile. We use ENVI-met model to simulate a metropolitan area with buildings, vegetation, paved surfaces, and traffic emissions to estimate air pollution abatement for varying building heights and coverage ratios of GRs and GWS. We simulate these layouts and coverage for a downtown area of Santiago, and results were compared with the base case scenario. Results showed that the air quality improvement by GRs and GWS depends on building height, surrounding urban infrastructure, vegetation cover and proximity to the pollutant source. Specifically, results showed that 50%–75% of GRs coverage on low-rise buildings could improve air quality at the pedestrian/commuter level. However, just a 25% coverage of GWS yields the highest PM_{2.5} capture. We conclude that to decrease PM_{2.5} concentrations, priority should be given to install GRs in buildings lower than 10 m in height. For GWS, the PM_{2.5} abatement is favorable in all cases. ENVI-met results also show that the combined use of GRs and GWS could reduce PM_{2.5} up to 7.3% in Santiago compared to the base case scenario.

1. Introduction

Urban air pollution is one of the crucial factors affecting public health for city residents. Exposure to polluted air has been associated with severe health problems that lead to high mortality rates, causing an estimated 7–10 million premature deaths per year worldwide [1,2]. Among different pollutants in the atmosphere, increased exposure to fine particulate matter (PM_{2.5}), with an aerodynamic diameter less than 2.5 μm , negatively impacts public health. PM_{2.5} is associated with severe

health problems that can lead to death [3,4] and childhood asthma [5].

Green infrastructures (GI) reduces pollutants through dry deposition and uptake through leaf stomata and is considered an effective mitigation strategy to improve urban air quality [6–8]. Recent studies have recognized the vital role of GI in sustainable and resilient urban planning [9]. Improvements related to the urban heat island effect, water runoff control, air quality, energy consumption, urban biodiversity are among the benefits of GI [10–14].

Specifically, numerous studies on improving urban air quality have

* Corresponding author. Department of Construction Engineering and Management, Pontificia Universidad Católica de Chile, Santiago, 7820436, Chile.
E-mail address: svera@ing.puc.cl (S. Vera).

Table 1

Past numerical studies used to evaluate urban air quality using different forms of GI.

Model	Simulation in	Pollutant	Modelling of	City	Author	Infrastructure
i-Tree	UFOR	PM ₁₀	Removal	Santiago, Chile	[35]	GRs, shrubs and grasses
	UFOR	NO ₂ , SO ₂ , CO, PM ₁₀ y PM _{2.5}	Removal	Melbourne, Australia	[16]	GRs, GWs and trees
Open FOAM	UFOR	NO ₂ , SO ₂ , CO, PM ₁₀	Removal	Toronto, Canada	[36]	GRs and shrubs
	CFD (Open source) + sink	PM _{2.5}	Concentration change	Leicester City (2 Km)	[37]	Trees and grass
Open FOAM	CFD (Open source) + sink	PM ₁₀	Concentration change	Antwerp, Belgium	[38]	Trees and grass
Open FOAM	CFD (Open source)	PM _{2.5} and NO _x	Concentration and deposition	Marylebone, UK	[17]	Trees
FLUENT	CFD (Open source)	PM ₁₀ and NO _x	Concentration (street intersection)	Bari in southern Italy	[39]	Trees
FLUENT	CFD (Open source)	PM ₁₀	Dispersion particles and concentration (wind tunnel)	Karlsruhe, Germany	[40]	Trees
RANS	CFD (Open source)	NO _x	Concentration (canyons)	The central region of Seoul, Korea	[41]	GRs
ENVI-met	CFD (close)	PM ₁₀	Concentration (canyons)	Strasbourg, France	[19]	Trees and hedges
RANS	CFD (Open source)	PM ₁₀ and NO _x	Concentration (canyons)	Mol, Belgium	[42]	Trees and hedges
WRF and ENVI-met	CFD (close)	PM ₁₀	Concentration air	Chicago city	[21, 32]	Green surfaces
			UHI-Concentrations PM Mesoscale: WRF Microscale: ENVI-met			
WRF	NOAA and NCEP	NO ₂ PM ₁₀ y O ₃	i-Tree + CMAQ + WRF = Vd, kg rem CMAQ: Community Multiscale Air Quality WRF + i-Tree = dispersion, concentration and Rem	Baltimore	[6]	Trees
PHOENICS	CFD	PM ₁₀	Concentration (canyons)	Florencia, Italia	[43]	Trees
				Beijing, China	[44]	GRs and GWs

focused on trees [15–19], grasses [16,17,20], shrubs [21–25], hedges [15,19,26], green roofs (GRs) [16,23,27–29] and green walls (GWs) [15, 23,29–31]. Benefits of trees in urban canyons are debatable. Rather than acting as a sink for air pollutants by particle deposition, trees in congested urban canyons may provide resistance to the canyon flows and reduce vertical mixing and local air circulation. Consequently, local PM concentration increases and urban air quality worsen [17,19,31]. Hedges closer to the pollutant source are a better alternative than trees in deep urban canyons due to their reduced capacity to modify canyon air circulation and mixing [19]. In open urban spaces (e.g., roadside), a combination of a solid barrier and a vegetation cover can help by controlling the outflow and dispersion of vehicular pollutants [26]. For open green urban spaces, low ecological landscaping is preferred to lower wind blocking by vegetation. Meanwhile, GRs and GWs provide minimum resistance to the flow over and around the buildings and are aesthetically appealing [21,32]. All these GI mitigation strategies can increase local ventilation, reduce urban heating and improve urban air

quality when properly deployed [33].

Numerical models have proven to be useful tools for evaluating the performance of GI mitigation strategies of urban air quality [16], and Table 1 summarizes such past numerical modeling studies. Interestingly, we were unable to locate any urban numerical studies on the combined effects of both GRs and GWs on air quality. In this paper we investigate the potential impact of urban GRs and GWs configurations, i.e., spatial layout and coverage, in reducing air pollution by capturing PM_{2.5} in the semiarid climate of Santiago, Chile. Here, the spatial layout refers to the location of GRs and GWs in the urban environment (i.e., GI is located in urban open spaces or street canyons), building height where GI is placed and the distance from the PM source. Coverage refers to the percentage of the available walls and roof building surfaces covered by GWs and GRs. Past studies have shown that the performance of GRs and GWs in capturing the PM varies with different plant species due to their varying morpho-physiological characteristics [23,34]. Most of the numerical models shown in Table 1 are only based on aerosol dynamics,

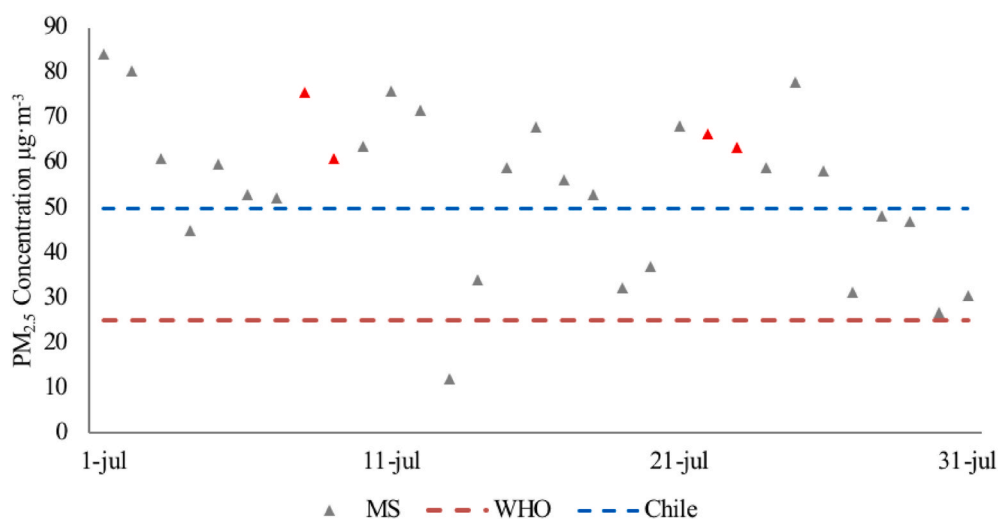


Fig. 1. Daily ambient PM_{2.5} concentrations in July 2015 (MS - Meteorological Station, grey triangles), WHO and Chilean PM_{2.5} standards.

Table 2

Summary of input, test parameters and corresponding values for validation model, sensitivity analysis and greener model.

Description	VM	SAM	GCM
Location	Santiago of Chile ($-33.47, -70.66$)		
Domain size	$90 \times 125 \times 20, 2$ $L (190 \text{ m} \times 250 \text{ m} \times 40 \text{ m})$	$120 \times 120 \times 30, 2$ $L (360 \text{ m} \times 360 \text{ m} \times 90 \text{ m})$	$274 \times 274 \times 50, 2 \text{ L}$ $(822 \text{ m} \times 822 \text{ m} \times 150 \text{ m})$
Building	$16 \text{ m} \times 60 \text{ m}; h: 12 \text{ m}$	Four blocks	Sixteen blocks
Grid resolution	$2 \text{ m} \times 2 \text{ m} \times 2 \text{ m}$ (x, y, z)	$2 \text{ m} \times 2 \text{ m} \times 2 \text{ m}$ (x, y, z)	$3 \text{ m} \times 3 \text{ m} \times 3 \text{ m}$ (x, y, z)
Start date	July 8, 9, 22 and 23; 4:00 h	July 23; 4:00 h	July 23; 6:00 h
Wind; RHmin; RHmax;	Meteorological Station of Independencia, Santiago, Chile, July 2015		
Source	CO; Line: from (DICTUC, 2016) $\mu\text{g}/\text{m} \cdot \text{s}$; rate: 600 s		
Surfaces	Concrete buildings; concrete pavement; loamy soil		
Green infrastructure	Grass; trees: <i>Platanus acerifolia</i> , <i>Robinia pseudoacacia</i> , <i>Palma washingtonia</i> and, <i>Sedum album</i>		
Run	12 h per day	4 h	3 h

disregarding the effect of morpho-physiological plant characteristics on dry deposition. This paper also accounts for PM dynamics and vegetation characteristics to provide recommendations for optimal configurations of GWs and GRs for urban planning.

2. Methods and numerical modeling description

We selected ENVI-met numerical model to study the impact of GRs and GWs on urban air quality. ENVI-met is a three-dimensional, non-hydrostatic computational fluid dynamics model for simulating urban environments [45]. Our assessment of studies in Table 1 shows that ENVI-met model advantages over other models. It treats vegetation by factoring in the plant's metabolism to analyze the performance of GRs and GWs in an urban environment. Specifically, ENVI-met considers particle dynamics, vegetation characteristics such as deposition velocity, leaf area index (LAI), and species-dependent metabolisms in simulating urban flows. These considerations are essential in experiment's design, as literature shows that the efficacy of GRs and GWs in capturing PM varies with plant species, due to varying morpho-physiological characteristics [23,34]. In addition, ENVI-met does not overly parameterize components of urban microclimate. It combines a Reynolds-averaged Navier-Stokes atmospheric model based on the Boussinesq approximation and a k- ϵ 1.5-order turbulence closure scheme with an explicit treatment of radiative fluxes, vegetation and soil. Multiplies studies have demonstrate that ENVI-met model is

capable of predicting meteorological variables [46–49] and species transport and concentrations [50] very well.

We selected downtown Santiago of Chile for our study, as it shows high levels of air pollution. Santiago's climate is Mediterranean [51], and the highest air pollution (Fig. 1) occurs in the winter season due to low mixing heights, weaker winds and strong thermal inversions enhanced by subsidence [49,52–54]. As a consequence, there is an accumulation of pollution in the lower boundary layer and city canyons such as those in the city center. We implemented the ENVI-met model to simulate a 16-blocks neighborhood in downtown Santiago (Fig. 6).

2.1. Research methodology

The design of experiments includes the development of three ENVI-met models called the Validation Model (VM), Sensitivity Analysis Model (SAM), and Greener Corridor Model (GCM). The VM was developed to validate the ENVI-met model based on estimating carbon monoxide (CO) as air pollutant. The SAM model includes four blocks of downtown Santiago. It was developed to identify the best GRs and GWs layout and coverage to be used in the GCM. Finally, the GCM includes sixteen blocks in downtown Santiago. It was designed to assess the influence of the urban layout and coverage of GRs and GWs on the air quality at a local urban scale. Table 2 shows a summary of the input parameters used for each ENVI-met model and Fig. 2 and Table 2 present the research methodology.

2.1.1. Validation model (VM)

To validate ENVI-met, we developed an idealized configuration to account for different surfaces and vegetation in our domain of interest of a Santiago's urban neighborhood (Fig. 3). Here, we performed four simulations for July 2015. All selected periods were highly polluted and exceeded WHO standards of ambient $\text{PM}_{2.5}$ concentration [55]. A representative sample was selected for a larger population [56] with 95% confidence $n = 48$, which is equivalent to 4 days, considering 12 h per day. The days were randomly selected for the month with the highest pollution levels in Santiago. Each experiment (highlighted with red triangle markers in Fig. 1) was performed for 12 h from 4:00 to 16:00 local time on 8, 9, 22 and July 23, 2015. Observed meteorological variables that influence the dispersion of pollutants, such as temperature, relative humidity (RH), and wind speed are shown in Fig. 4. The simulated hourly CO concentration was compared with the closest CO monitoring station called Independencia Meteorological Station (MS). We selected CO as an inert tracer pollutant to validate our ENVI-met model and simplified proxy of $\text{PM}_{2.5}$ pollution in Santiago. This selection of CO as a surrogate in our design of experiments was based on the

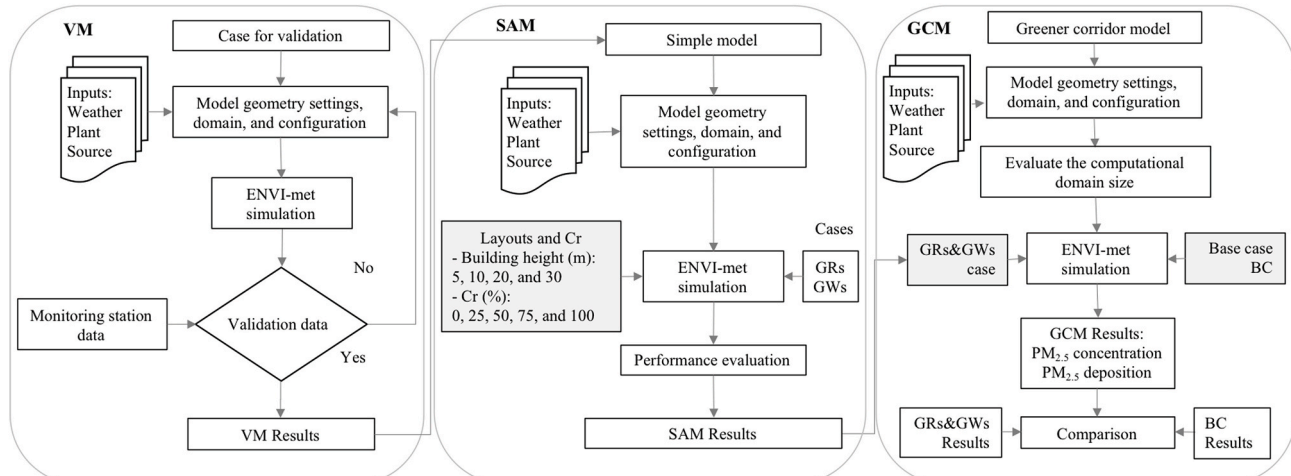


Fig. 2. Schematic representation of the research methodology.

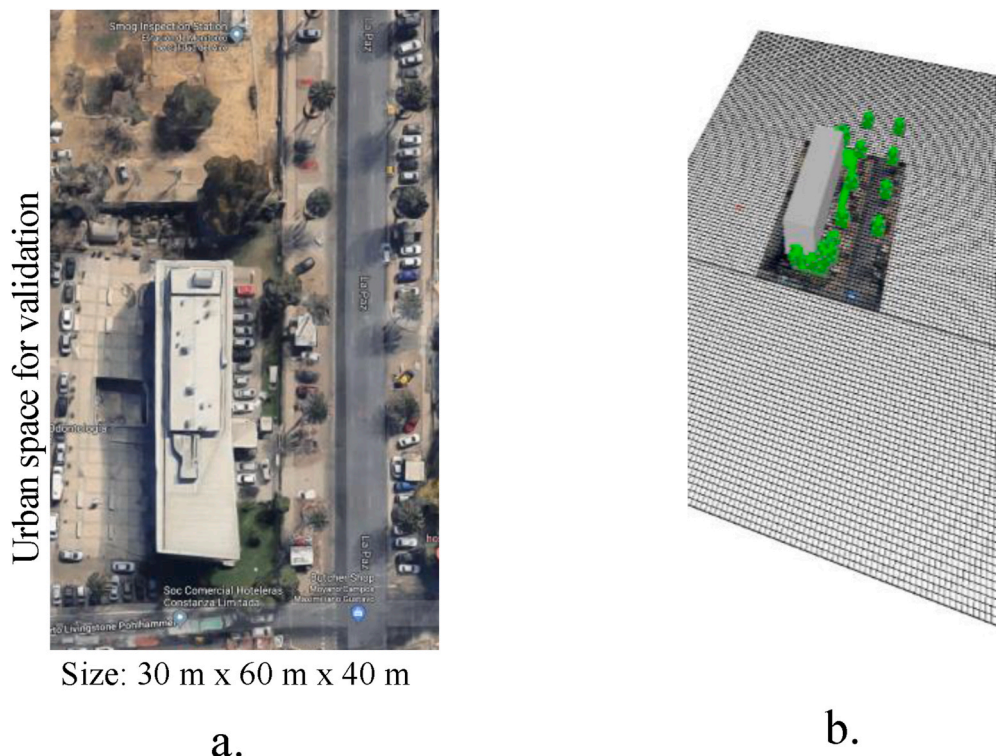


Fig. 3. Visualization of model domain in validation stage. a. Real image from Google Earth, 2018. b. Visualization in ENVI-met.

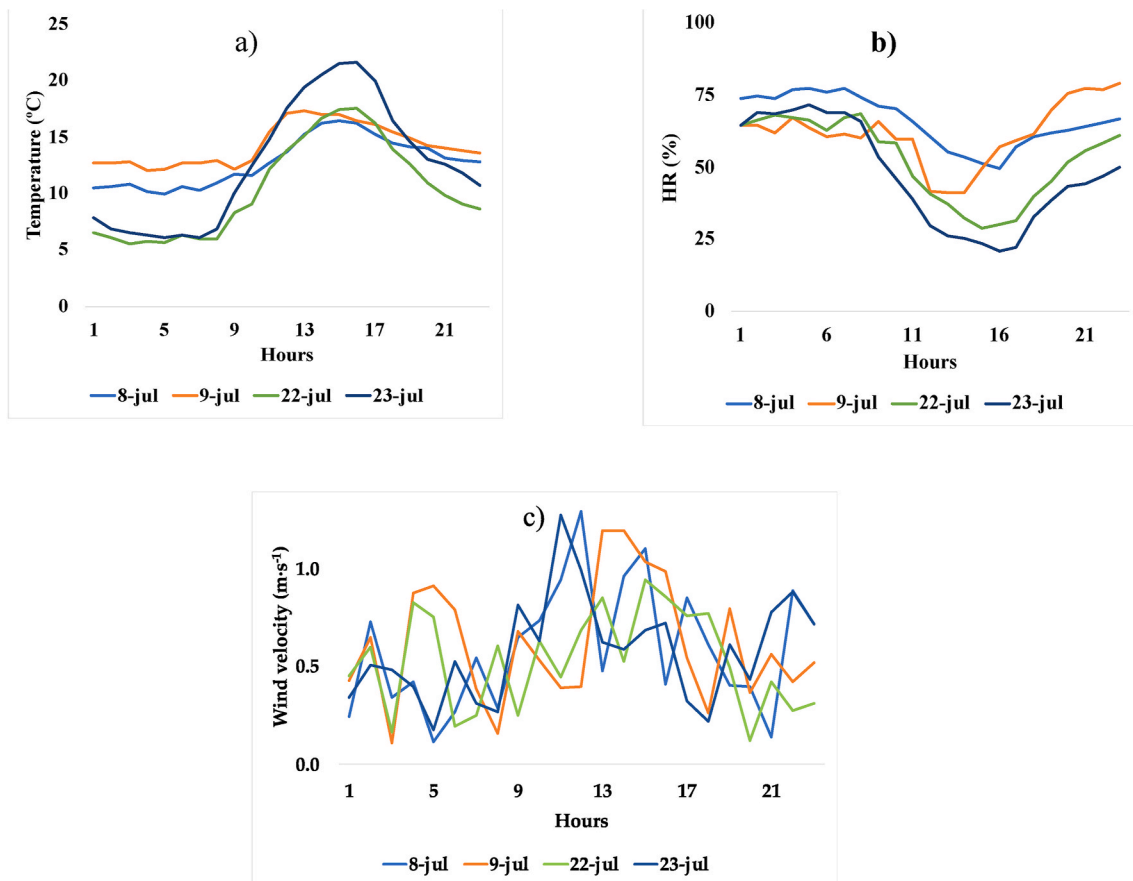


Fig. 4. Meteorological parameters from Independencia Meteorological Station: (a) temperature, (b) RH, and (c) wind velocity.

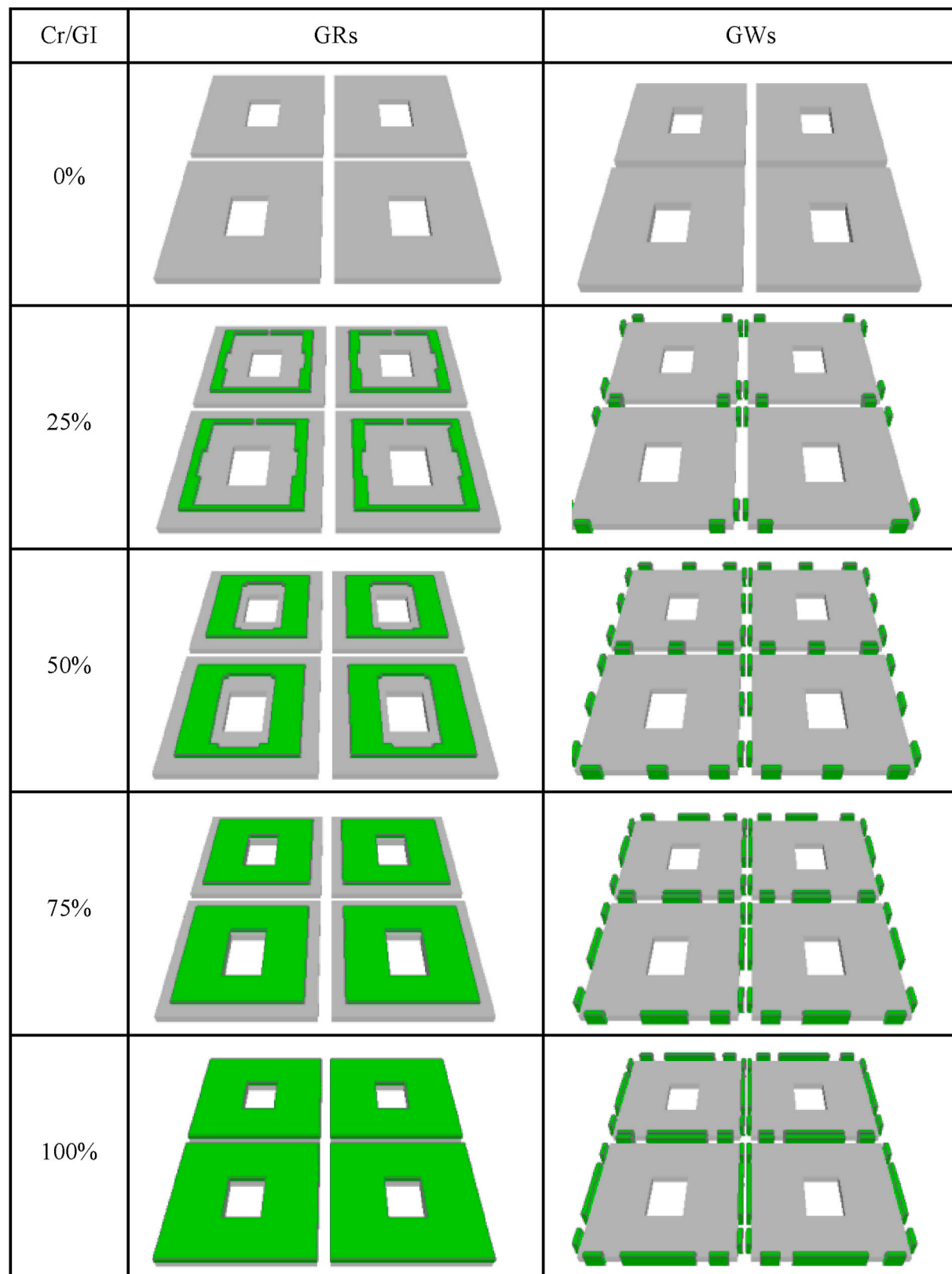


Fig. 5. Cr in green spaces layout for GRs and GWs sensitivity analysis. (For interpretation of the references to colour in this figure legend, the reader is referred to the Web version of this article.)

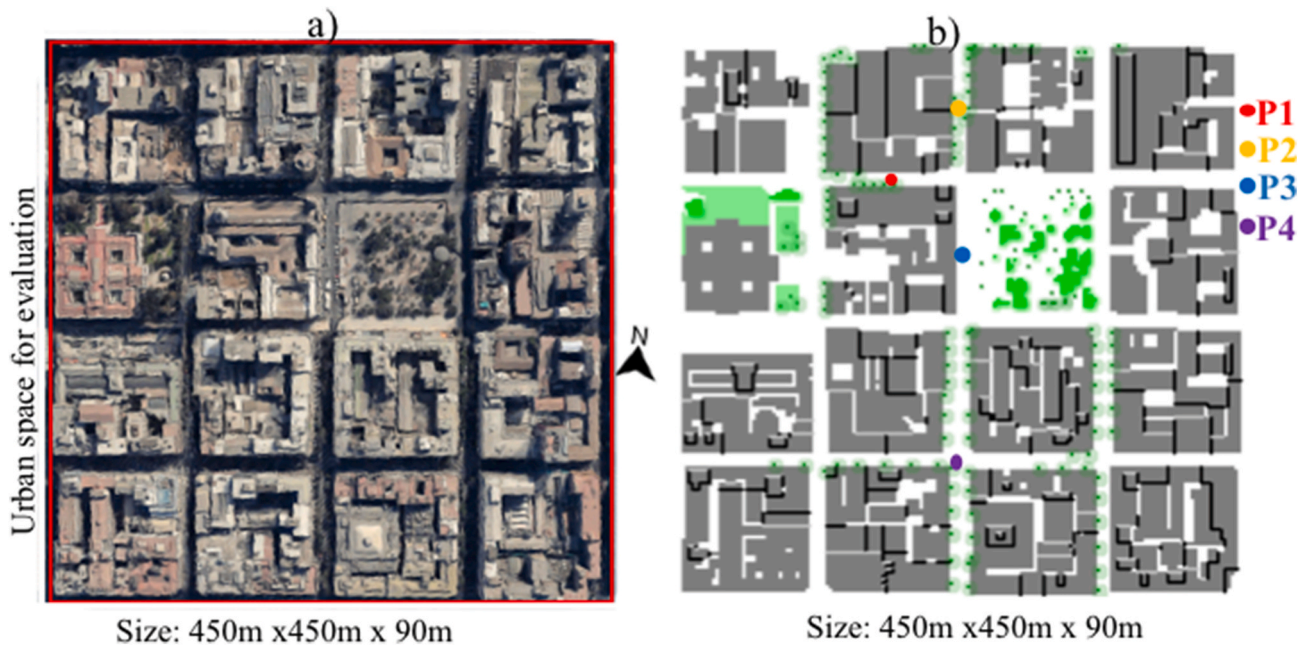


Fig. 6. Visualization of the green corridor case study, base scenario. a. Satellite images. b. ENVI-met model (plant view) showing locations of analysis P1, P2, P3 and P4. (For interpretation of the references to colour in this figure legend, the reader is referred to the Web version of this article.)

following rationale. (a) Unfortunately, Santiago lacks in a reliable pollution inventory for $PM_{2.5}$. Previous studies have illustrated that in the absence of long-range transport, $PM_{2.5}$ is mainly contributed by local traffic sources (vis-à-vis PM_{10} that is comprised of smoke and dust from industrial processes, agriculture, construction, road traffic, plant pollen and other natural sources), and (b) while $PM_{2.5}$ can be produced as secondary aerosols originating from fine sulphates and nitrates, according to previous studies discussed below, on urban scales where ENVI-met is applied, the contributions of all $PM_{2.5}$ (primary and secondary) is mainly contributed by transportation (combustion sources). Thus, there should be a significant relationship between combustion biproducts $PM_{2.5}$ and CO. In addition, recent studies over Africa [57], Guangzhou city and Pearl River Delta region in China [58], Phoenix, Arizona and UM/Mexico border [59,60], and Santiago [53,61] itself, suggest that there is a strong correlation between $PM_{2.5}$ and CO.

Thus, CO is a simplified proxy of $PM_{2.5}$ pollution in Santiago due to traffic emissions [53], and helps circumvent the challenges due to lack of a full pollution inventory for the area that is imperative for accurately simulating chemical reactions. Both $PM_{2.5}$ and CO are emitted simultaneously from traffic, the dispersion of both pollutants is well accounted in the simulations. Note, we do not capture $PM_{2.5}$ transformation due to chemical processes (e.g., secondary particulate matter) because the paper's main goal is to assess the potential of ambient $PM_{2.5}$ capture by GWs and GRs, so it is immaterial how the ambient $PM_{2.5}$ is setup into the modeling domain (by emissions, advection or chemical reactions).

2.1.2. Sensitivity analysis for ambient $PM_{2.5}$ (SAM)

To identify urban layouts and coverage of GRs and GWs for maximum capture of $PM_{2.5}$ in an urban environment, two cases, one for GRs and another for GWs, were considered, 4 h of simulation each. A sensitivity analysis evaluated the effect of GRs and GWs layout and urban coverage on $PM_{2.5}$ capture. The layout refers to the location of GRs and GWs on the buildings. Four building heights were considered (5 m, 10 m, 20 m and 30 m). Therefore, GRs are located according to the building height, and GWs cover the whole opaque wall façade along the building height. Additionally, five surface coverage ratios (Cr) of GRs and GWs are analyzed, 0%, 25%, 50%, 75%, and 100%. For GRs, a Cr of 100% corresponds to installing GRs on the total available free area of

building roofs, which means that the surface occupied by air conditioning system components and other elements on the roofs are not considered as part of the Cr. The free and occupied roof surfaces were identified with 2018 Google Earth images. Similarly, for GWs, Cr of 100% considers only the available wall surface of buildings to install GWs, excluding windows and doors. Fig. 5 shows the simulation domain of four blocks of Santiago's downtown; different layouts of GWs and GRs and the studied coverage areas used for SAM are identified. For this experiment, we analyzed ENVI-met modeled $PM_{2.5}$ concentrations at the pedestrian height (1.5 m). Large urban populations are exposed to higher air pollution while walking, biking, or commuting in a city, especially during rush hours when traffic emissions and ambient pollutants concentrations are the highest.

2.1.3. Greener Corridor Model (GCM)

Sixteen blocks in downtown Santiago were considered in this case study, as shown in Fig. 6. It included real buildings, pavement surfaces and GI, including trees. The 3D urban morphology model was created using 2018 satellite images from Google Earth. The different materials included in the model were: concrete for buildings, asphalt for the pavement surfaces, and soil and vegetation in the study domain. The input parameters of GCM are presented in Table 2. Simulations were performed for two scenarios: (1) the base case scenario (BC) that represents the current urban morphology, and (2) the green corridor case with hypothetical GRs and GWs on the buildings. We considered SAM results to identify the optimal layout and coverage of GRs and GWs (Section 3.2). We computed the total $PM_{2.5}$ deposition in the whole domain and identified four points to analyze the profile of concentrations: P1 is located inside the urban canyon with trees and GRs; P2 is inside of canyon with trees, GRs, and GWs; P3 is in a street interception, and P4 is located in an open space (Fig. 6).

2.1.4. Pollution source

$PM_{2.5}$ and CO emissions were computed from an equilibrium transport model of the city of Santiago, which simulates an urban transport system considering the capacity of roads and vehicles and the commuters' trip demand spatially distributed across the city [62]. This equilibrium flow model treats every workday alike. Therefore, the estimated emissions are the same for Monday through Friday for

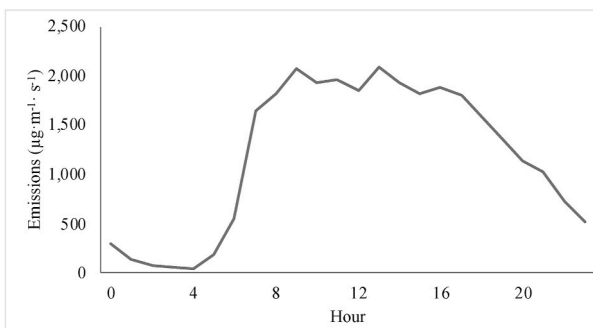


Fig. 7. CO emissions used in the model (DICTUC, 2016).

Santiago's transportation network. The background CO concentration for the ENVI-met simulations was equal to the lowest CO concentration between 1 a.m. and 4 a.m., when traffic very low. Fig. 7 shows the typical traffic CO emission used for VM, SAM, and GCM.

2.1.5. Vegetation

The urban vegetation (e.g., trees, grasses, and shrubs) included in VM and GCM closely represent the actual vegetation found at the study site. For GRs and GWs, we used *Sedum album* vegetation type. This species was selected taking into account the results previously reported by Viecco et al. [23], that investigated the capture of PM₁₀ and PM_{2.5} of nine species of plants used in GRs and GWs in Santiago. They concluded that *Sedum album* showed the highest potential for capturing PM₁₀ and PM_{2.5}. Other relevant variables for vegetation used in ENVI-met model were the Leaf Area Index (LAI) of 0.89 m³ m⁻³, a PM_{2.5} deposition velocity of 0.23 cm s⁻¹ [23], and 0.15 as albedo [63]. These variables were measured under laboratory conditions and are adjusted to the vegetation selected here.

3. Results and discussions

3.1. Validation of ENVI-met model

Fig 8 and 9 show that the simulated CO concentrations for VM agree well with the observations at the Independencia Meteorological Station (MS). Statistical analysis showed a positive linear correlation with an R-

square of 0.61 between hourly VM results and Independencia MS. These results reflect that our model setup can account for the turbulent transport of CO in a relatively small domain. Note, this approximation included only CO as a pollutant from traffic exhaust, even though in the real world, multiple types of contaminants from different combustion sources exist. Saide et al. (2011) showed CO-PM_{2.5} correlation coefficient as high as 0.95 using WRF-Chem CO tracer model study over Santiago [61]. Thus, we can assume that the surrogacy between CO and PM_{2.5} is viable whether chemical reactions are considered or not. The ENVI-met model results in this section show high correlation coefficients and trends between measured and modeled CO. Thus model results for PM_{2.5} can be used for making inferences without validation. (Note, the region lacks PM_{2.5} observations and inventory.) Thus, our ENVI-met model experimental design provides a robust setup that estimates reliably pollutants transport phenomena and concentrations of CO and PM_{2.5} for Santiago and a template for regions lacking in PM_{2.5} measurements and inventory.

Notice that Fig. 8 presents a reasonably stringent test for any dynamical air pollution model — see [64], for examples — because simulated and observed data are paired in time and space. The scattering of points around the regression line may be ascribed to a) weekly variability in actual emissions, b) advection of CO from nearby — not modeled — roads, c) vertical mixing with urban background air. The best agreement between simulated and monitored CO concentrations of the VM was on July 9 and 23 (Fig. 8 (b) and 8 (d)). On the other hand, results for July 8 and 22 (Fig. 8 (a) and 8(c)) showed lower agreement. This could be explained because the model considers only transport emissions related to work-home trips, and it does not include small-scale factors like commercial activity around the zone. For example, close to the study area, each Wednesday, a free marketplace is installed, which could increase the levels of pollutants recorded at the monitoring station due to extra freight and shopping activities.

3.2. Sensitivity analysis from SAM

Fig 10 and 11 show the percentage variation of PM_{2.5} concentration for different coverage ratios (Cr) for GRs and GWs, respectively. GRs cause the highest reduction in PM_{2.5} concentrations for building heights of 5 and 10 m (Fig. 10). While PM_{2.5} concentration is reduced 3.7% for 100% Cr of GRs in buildings with 5 m height (Fig. 10a), a reduction of 2.7% of PM_{2.5} concentration is observed in building with 10 m height

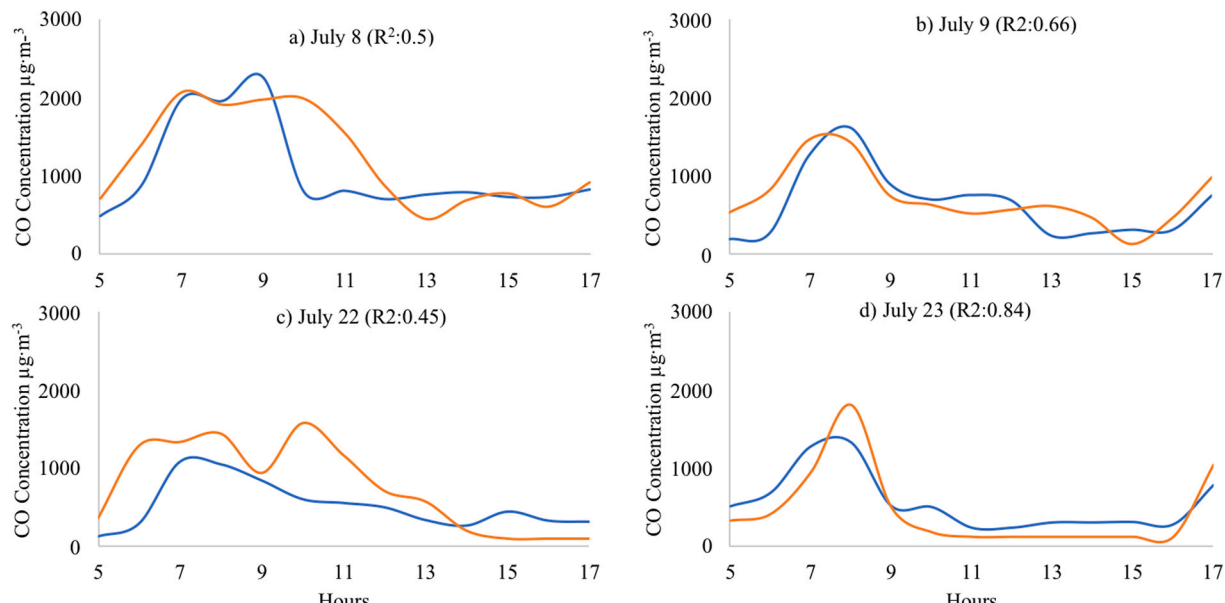


Fig. 8. VM and Independencia MS daily CO concentrations four days in July.

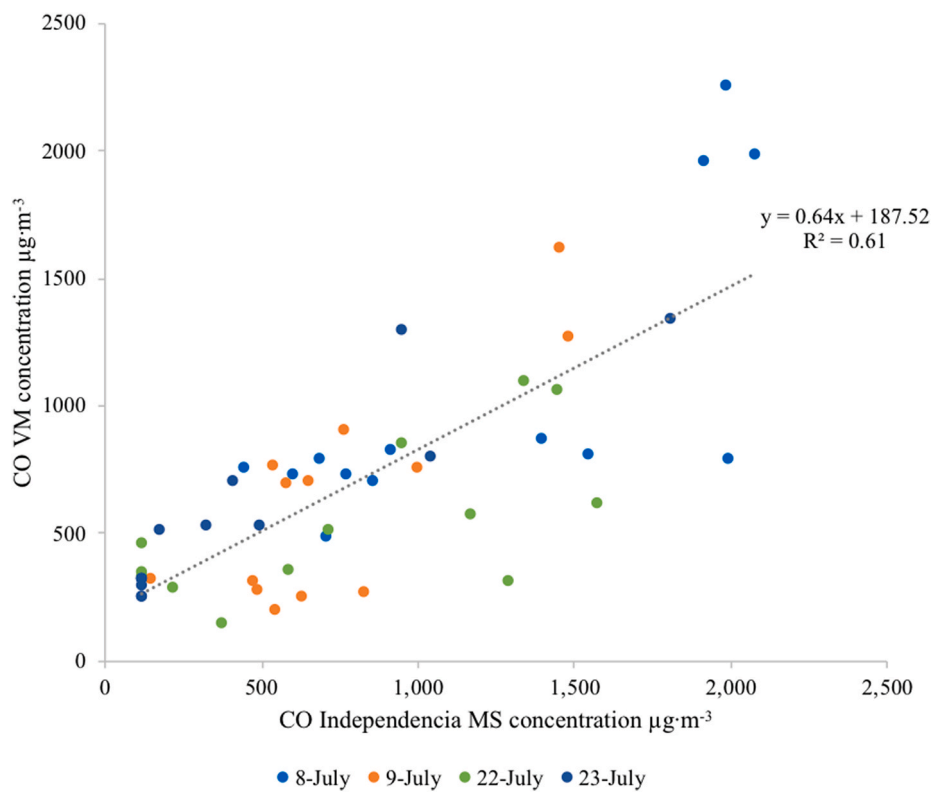


Fig. 9. Correlation between VM and Independencia MS CO concentrations.

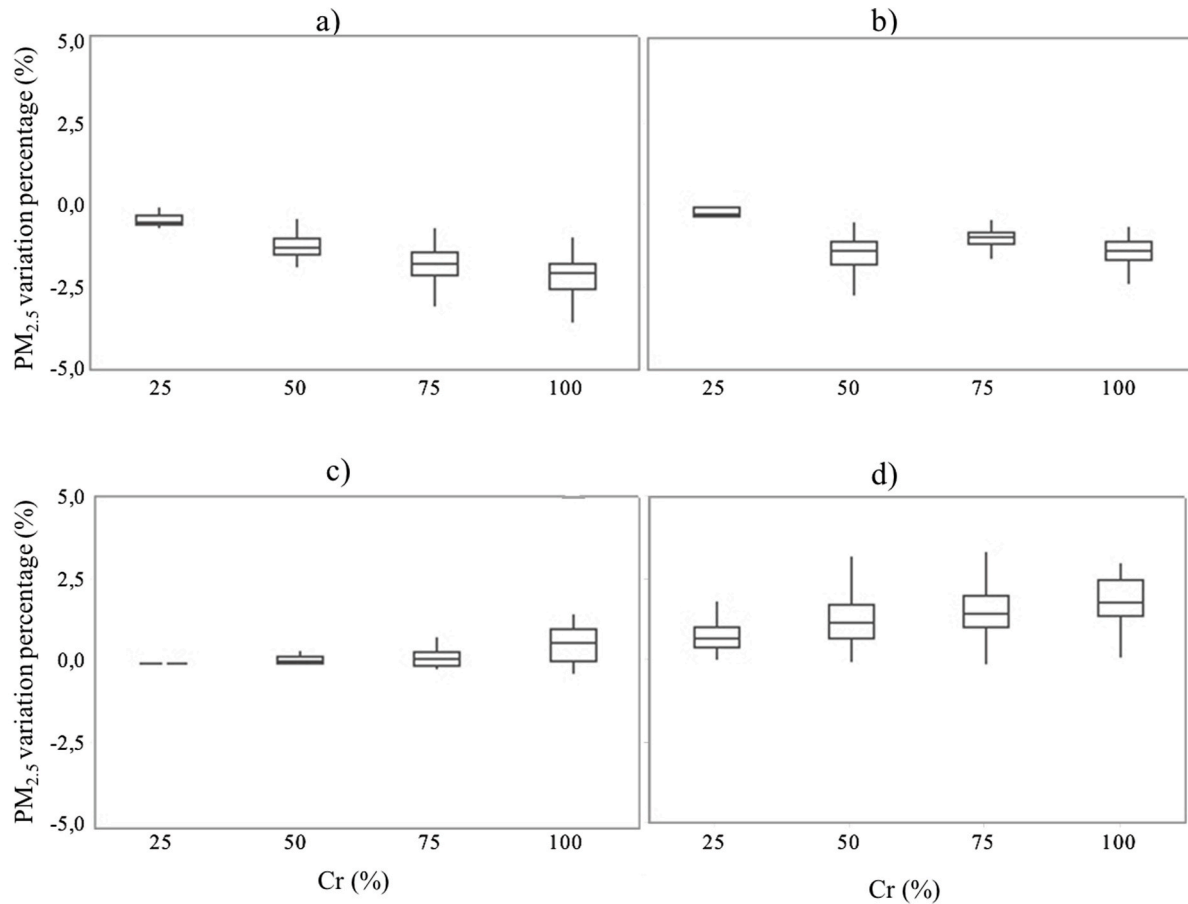


Fig. 10. PM_{2.5} percentage variation with different coefficient ratio Cr in green roofs GRs at the pedestrian level. Height: a) 5 m, b) 10 m, c) 20 m and d) 30 m

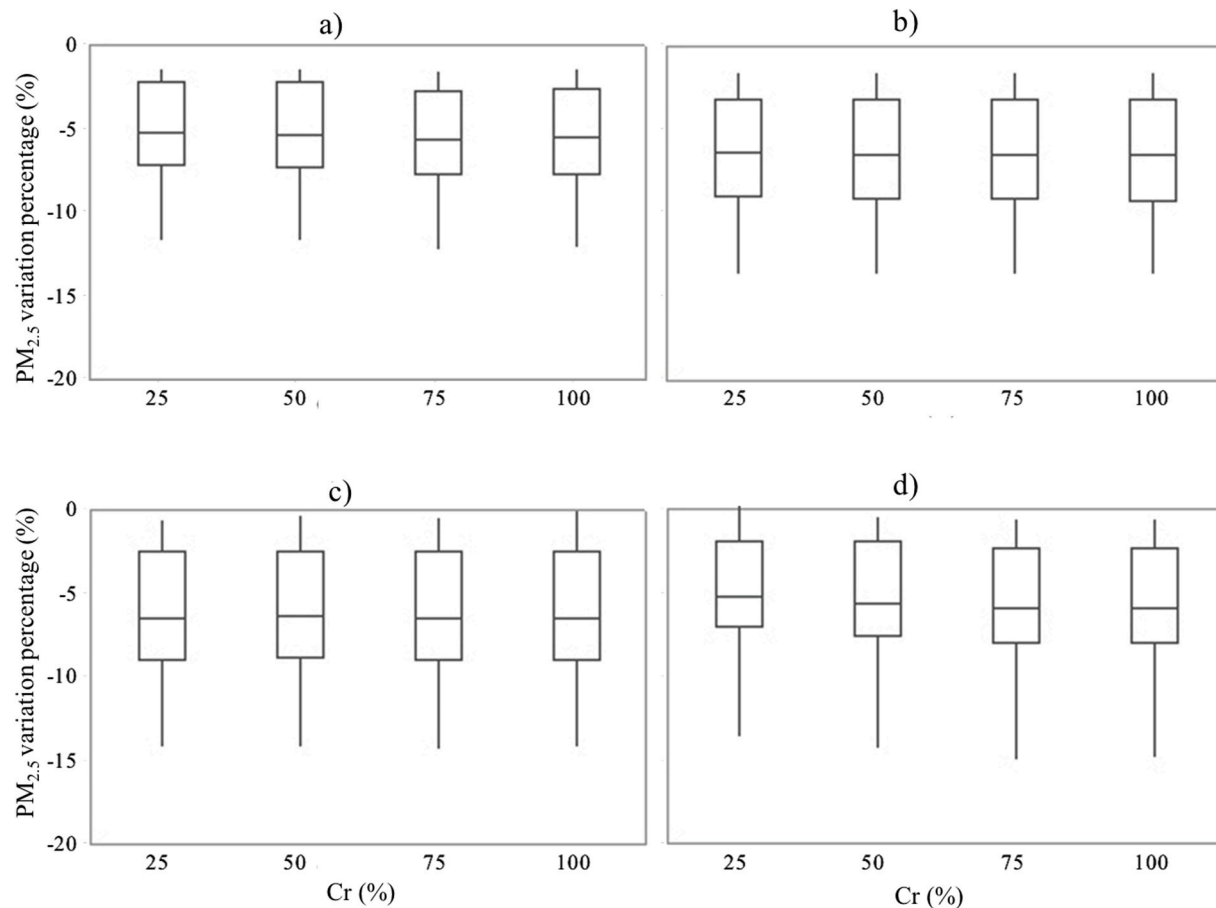


Fig. 11. $\text{PM}_{2.5}$ percentage variation with different coefficient ratio Cr in GWs at the pedestrian level. a) 5 m, b) 10 m, c) 20 m and d) 30 m.

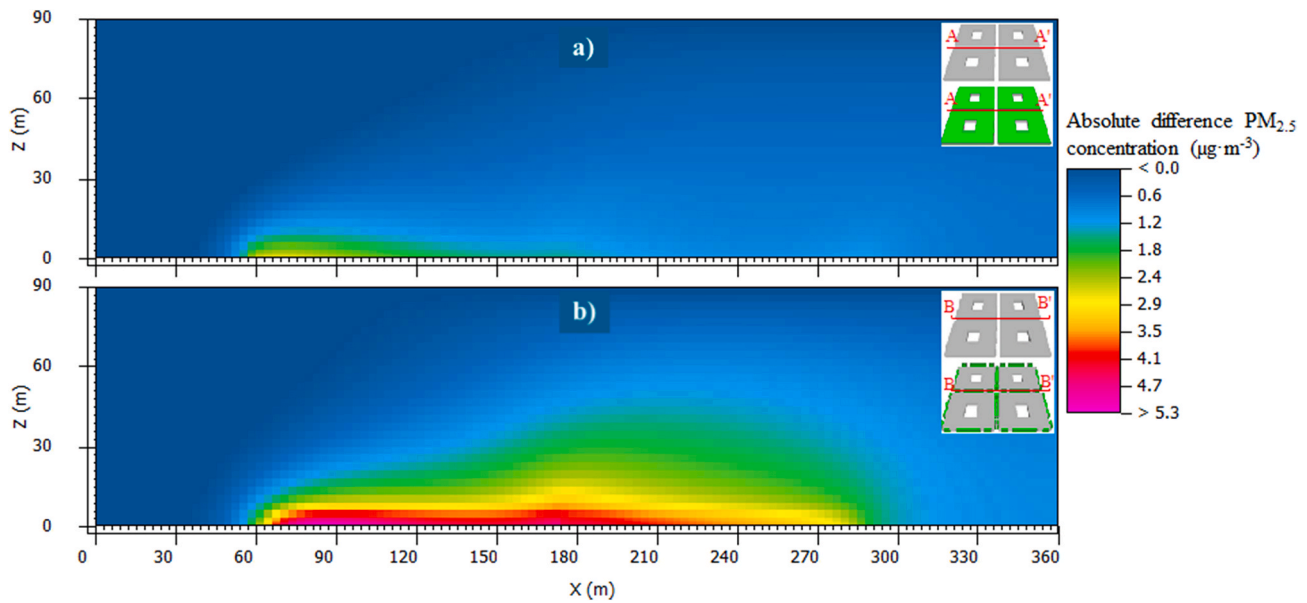


Fig. 12. Variation $\text{PM}_{2.5}$ concentration profile inside a street for buildings with 5 m height. a) GRs SAM Cr 100% versus Cr 0% A-A'. b) GWs SAM Cr 100% versus Cr 0% B-B'.

and 100% Cr (Fig. 10b). On the other hand, GRs at buildings heights of 20 and 30 m did not improve air quality at the pedestrian level. Also, Cr of 75% and 50% GRs at building height of 5 m and 10 m, respectively, causes as much $\text{PM}_{2.5}$ concentration decrease as Cr of 100% at the same

height. Therefore, the reductions in $\text{PM}_{2.5}$ concentration with GRs are dependent on the height that the GRs are located and Cr.

While GWs show a reduction in $\text{PM}_{2.5}$ concentration up to 15% for all cases (Fig. 11), higher Cr values show marginal improvements in $\text{PM}_{2.5}$

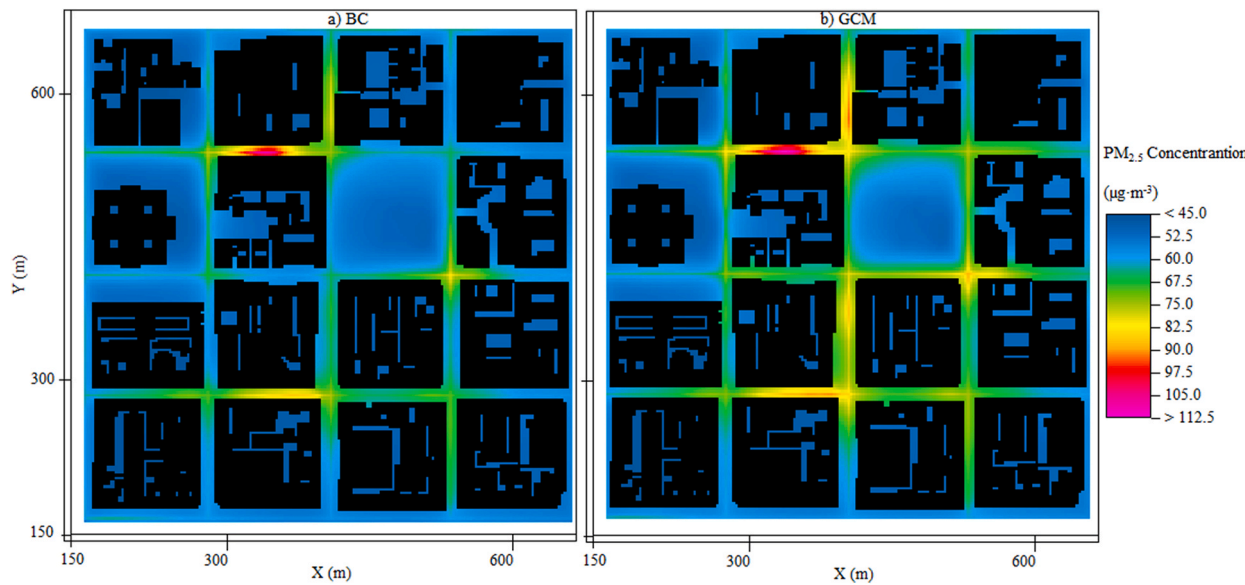


Fig. 13. PM_{2.5} concentrations in the urban environment for two cases:a) BC and b) GCM.

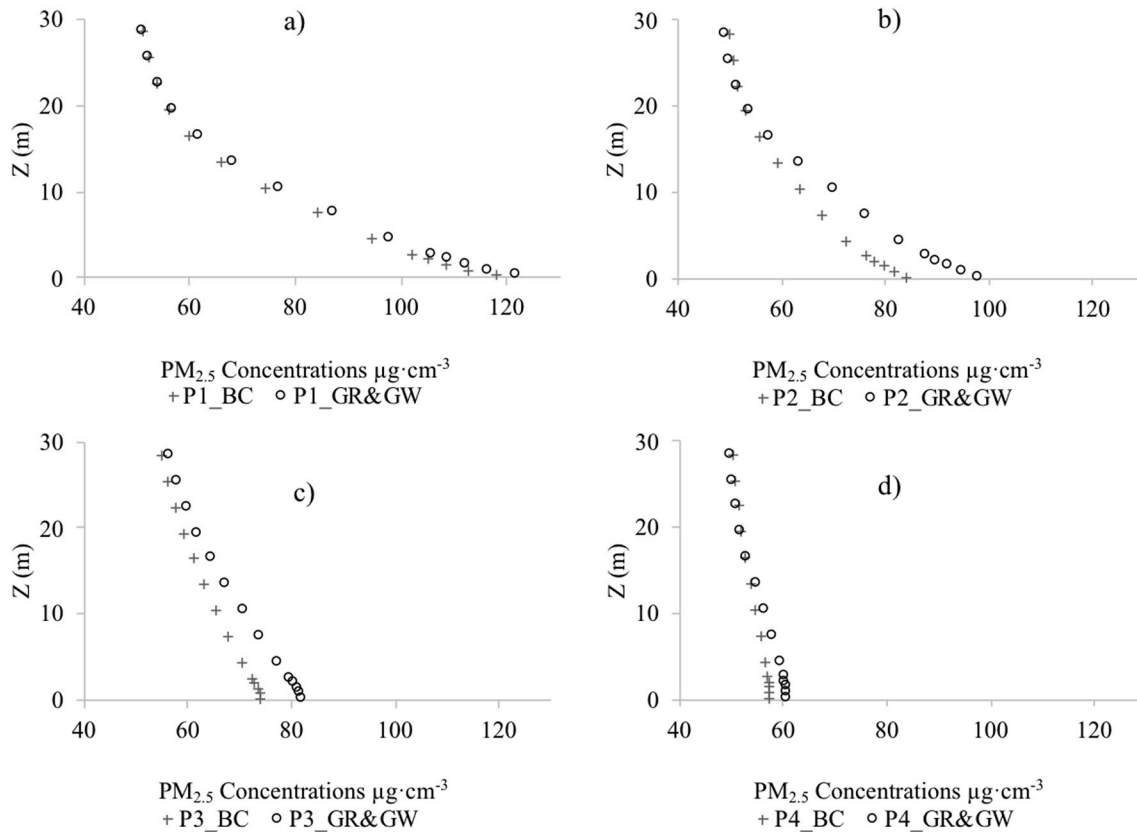


Fig. 14. Profile of PM_{2.5} concentrations for base case (BC) and GCM (GR&GW) in four points: a) P1 inside of canyon with trees and green roofs GRs; b) P2 inside of canyon with trees, green roofs GRs and green walls GWs; c) P3 an interception and d) P4 in an open space.

concentration. Simulation results showed that Cr of 25% is optimum to improve air quality at the pedestrian level by GWs.

Fig. 12 (a) shows PM_{2.5} concentrations for cases with 100% and 0% Cr inside a street, according to cross sections A-A' (GRs) and B-B' (GWs). The highest pollutant levels are inside the street canyons, and the concentration decreases away from the source. Thus, GRs works best in low-rise buildings. Comparing the results of Fig. 12a and b, we found that GWs are more effective than GRs to reduce PM_{2.5} concentration due to

the proximity of vegetation to the emission source and larger GWs surface area.

3.3. Influence of GRs and GWs on urban air pollution mitigation

This section presents the influence of GRs and GWs on the air quality of green corridor case study (GCM). Two types of results are shown, PM_{2.5} concentrations and PM_{2.5} depositions on GWs and GRs for the

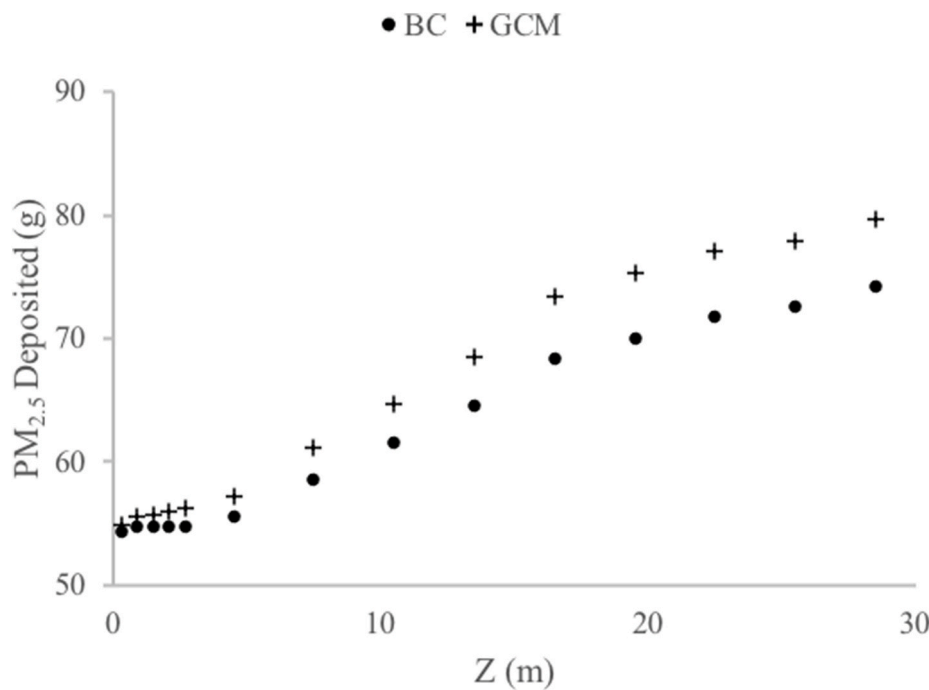


Fig. 15. Profile of PM_{2.5} deposited on all surfaces for BC and GRs and GWs.

GCM and base case (BC - without GRs and GWs).

Fig. 13 shows PM_{2.5} concentration at 1.5 m height (pedestrian/commuter level) between the base case (BC) and GCM. Overall, the PM_{2.5} concentrations at the pedestrian/commuter level did not decrease with GWs and GRs for 3 h. We identified four points to analyze the concentration profiles (see: methodology above).

With the presence of trees, GRs, and GWs, ENVI-met model showed an increase in PM_{2.5} concentration profiles in P1 (Fig. 14a) at the pedestrian level, likely due to an increase in roughness and a decrease in canyon wind speeds. Here the aerodynamic (drag) effects prevailing over the deposition effects. Dense trees in street canyons likely have a negative impact on PM_{2.5} due to reductions in air circulation and decreasing low-level turbulence. These findings agree with other studies that investigated the effect of trees in street canyons [17,33]. Therefore, we suggest GRs only in canyons, and installation of GWs should be done with caution. Besides, ENVI-met simulations showed that trees in urban canyons do not improve urban air quality, although they are known for environmental and social benefits (e.g., Heat Island reduction). Fig. 14b shows that the rate of decrease per unit meter of height was 42% more for GRs and GWs than that for the BC. Similar effect was found at the street intersection P3 and the open space P4. The PM_{2.5} concentrations with GRs and GWs were 35% and 57% higher than the concentration of the BC (Fig. 14c and d).

On the other hand, comparing PM_{2.5} depositions at all the surfaces of the model, the case with GRs and GWs demonstrates better performance than the BC, in that GRs and GWs increase the capture of PM_{2.5} by 7.3% compared to BC. The deposition results show that the highest deposition levels are between 7.5 m and 16.6 m (Fig. 15). This result agrees with Ottel et al. (2010) who concluded that the proximity to the source increases PM_{2.5} deposition on vegetation. This result means GRs and GWs could remove up to 7.3% of PM_{2.5} from polluted air compared with the urban morphology of the BC. Finally, we note that a positive impact of PM_{2.5} depositions in GCM was found due to a larger deposition surface and increased residence times within the street canyons that enhances deposition. Nevertheless, changes in PM_{2.5} concentration was non-uniform throughout the simulated urban domain and were dependent on meteorology.

4. Conclusions and recommendations

We implemented an ENVI-met model over a Santiago's urban neighborhood and evaluated multiple scenarios of green roofs and green walls. This study was constrained by the lack of a pollution inventory. We used available nearest CO station measurements as a surrogate for PM_{2.5} emitted (or precursors are emitted) due to transportation. We caution the readers to exercise circumspection when interpreting results of the manuscript due to this limitation. Note, as highlighted in Section 2 on Methods and Section 3 on Results, such proxy studies are valuable for heat, air quality, and flood mitigation assessment studies that could inform decisions to make developing cities and communities lacking in extensive observations more sustainable and resilient.

The main conclusions of this paper are the following:

- GWs have a more significant impact than GRs for improving air quality. Based on SAM results, the proximity of GRs and GWs to the emission source and green coverage ratio (Cr) are key factors underlying improved air quality at the pedestrian/commuter level, which should be considered in urban design and planning. The results showed that PM_{2.5} concentrations are reduced by 3.7% and 2.7% for buildings with GRs and heights of 5 m and 10 m, respectively. On the other hand, PM_{2.5} concentration decreases up to 15% for GWs.
- Coverage ratio (Cr) of GRs and GWs is a key factor determining the performance of PM_{2.5} capture of GRs and GWs in an urban area. We found that the optimum PM_{2.5} capture does not occur at Cr = 100%. This means that optimum Cr values must be evaluated based on simulations for specific traffic and urban morphology.
- GRs and GWs remove up to 7.3% of PM_{2.5} from polluted air based on the GCM. The implementation of GRs and GWs at the same time has a positive impact on PM_{2.5} deposition.

Based on the above research, the following recommendations are proposed for the use of GWs and GRs in urban planning and design of downtown Santiago, Chile to mitigate air pollution by fine particle matter:

- Priority should be given to installation of GRs in buildings lower than 10 m height. For GWs, the effect is more extensive in all cases because they are installed on the building façade exposed to traffic.
- The Coverage ratio (Cr) should be 75% and 50% for GRs on buildings of 5 and 10 m height, respectively. While for GWs, a Cr of 25% is suggested for all cases.
- Dense trees in street canyons combined with GWs should be avoided because trees cause a reduction of air circulation and a consequent increase of PM_{2.5} concentrations that lead to deterioration of air quality at the pedestrian level.

The above quantitative findings and recommendations are specific to GRs and GWs implementations in Santiago, Chile. However, the presented results could guide urban planning for cities with similar climate and urban morphology, and the research methodology is portable to other cities lacking in exhaustive emission inventory. Finally, GRs and GWs are excellent choices to mitigate air pollution in urban environments, especially when GRs and GWs are placed strategically to obtain the best coverage area, proximity to the source of exposure, location with respect to surrounding buildings and other existing GI.

Author contributions

M.V., H.J.S. and S.V. conceived and designed the experiments; M.V. done simulations; all authors analyzed the data and contributed to writing of the paper.

Declaration of competing interest

The authors declare that they have no known competing financial interests or personal relationships that could have appeared to influence the work reported in this paper.

Acknowledgements

This work was funded by the research grant FONDEF ID15I10104 of the National Commission for Science and Technological Research (CONICYT) of Chile, and supported by the Center for Sustainable Urban Development (CEDEUS) through the project CONICYT/FONDAP/15110020, National Doctoral Scholarships CONICYT 21182050 Academic Year 2018, and VRI-CPD 2017 Scholarships. Ashish Sharma was also partially supported by the Illinois State Water Survey, Prairie Research Institute at the University of Illinois, Urbana-Champaign.

References

- [1] WHO, 7 Million Premature Deaths Annually Linked to Air Pollution, World Health Organization, Geneva, Switzerland, 2014.
- [2] P.M. Manzucci, M. Franchini, Health effects of ambient air pollution in developing countries, *Int. J. Environ. Res. Publ. Health* 14 (2017) 1048.
- [3] J.O. Anderson, J.G. Thundiyil, A. Stolbach, Clearing the air: a review of the effects of particulate matter air pollution on human health, *J. Med. Toxicol.* 8 (2012) 166–175, <https://doi.org/10.1007/s13181-011-0203-1>.
- [4] C.A. Pope III, R.T. Burnett, M.J. Thun, E.E. Calle, D. Krewski, G.D. Thurston, Lung cancer, cardiopulmonary mortality, and long-term exposure to fine particulate air pollution, *J. Am. Med.* 287 (2002) 1132–1141.
- [5] R. Dimitrova, N. Lurpongulakana, H.J.S. Fernando, G.C. Runger, P. Hyde, B. C. Hedquist, J. Anderson, W. Bannister, W. Johnson, Relationship between particulate matter and childhood asthma—basis of a future warning system for central Phoenix, *Atmos. Chem. Phys.* 12 (2012) 2479–2490.
- [6] M.T.I. Cabrabalan, C.N. Kroll, S. Hirabayashi, D.J. Nowak, Modeling of air pollutant removal by dry deposition to urban trees using a WRF/CMAQ/i-Tree Eco coupled system, *Environ. Pollut.* 176 (2013) 123–133, <https://doi.org/10.1016/j.envpol.2013.01.006>.
- [7] J. Yang, Q. Yu, P. Gong, Quantifying air pollution removal by green roofs in Chicago, *Atmos. Environ.* 42 (2008) 7266–7273, <https://doi.org/10.1016/j.atmosenv.2008.07.003>.
- [8] M. Tallis, G. Taylor, D. Sinnett, P. Freer-Smith, Landscape and Urban Planning Estimating the removal of atmospheric particulate pollution by the urban tree canopy of London, under current and future environments, *Landsc. Urban Plann.* 103 (2011) 129–138, <https://doi.org/10.1016/j.landurbplan.2011.07.003>.
- [9] A. Sharma, S. Woodruff, M. Budhathoki, A.F. Hamlet, F. Chen, H.J.S. Fernando, Role of green roofs in reducing heat stress in vulnerable urban communities—a multidisciplinary approach, *Environ. Res. Lett.* 13 (2018) 94011.
- [10] D. Wuebbles, A. Sharma, A. Ando, L. Zhao, C. Rigsbee, Converging on Solutions to Plan Sustainable Cities, *Eos, Washington, DC*, 2020, p. 101, <https://doi.org/10.1029/2020EO150149>.
- [11] F. Victorero, S. Vera, W. Bustamante, F. Tori, C. Bonilla, J. Gironás, V. Rojas, Experimental study of the thermal performance of living walls under semiarid climatic conditions, *Energy Procedia* 78 (2015) 3416–3421.
- [12] J. Herrera, G. Flamant, J. Gironás, S. Vera, C.A. Bonilla, W. Bustamante, F. Suárez, Using a hydrological model to simulate the performance and estimate the runoff coefficient of green roofs in semiarid climates, *Water* 10 (2018) 198.
- [13] S. Vera, C. Pinto, P.C. Tabares-Velasco, W. Bustamante, F. Victorero, J. Gironás, C. A. Bonilla, Influence of vegetation, substrate, and thermal insulation of an extensive vegetated roof on the thermal performance of retail stores in semiarid and marine climates, *Energy Build.* 146 (2017) 312–321, <https://doi.org/10.1016/j.enbuild.2017.04.037>.
- [14] S. Vera, C. Pinto, F. Victorero, W. Bustamante, C. Bonilla, J. Gironás, V. Rojas, Influence of plant and substrate characteristics of vegetated roofs on a supermarket energy performance located in a semiarid climate, *Energy Procedia* 78 (2015) 1171–1176.
- [15] K.V. Abhijith, P. Kumar, J. Gallagher, A. McNabola, R. Baldauf, F. Pilla, B. Broderick, S. Di Sabatino, B. Pulvirenti, Air pollution abatement performances of green infrastructure in open road and built-up street canyon environments – a review, *Atmos. Environ.* 162 (2017) 71–86, <https://doi.org/10.1016/j.atmosenv.2017.05.014>.
- [16] V.M. Jayasooriya, A.W.M. Ng, S. Muthukumaran, B.J.C. Perera, Green infrastructure practices for improvement of urban air quality, *Urban For. Urban Green.* 21 (2017) 34–47, <https://doi.org/10.1016/j.ufug.2016.11.007>.
- [17] A. Jeanjean, R. Buccolieri, J. Eddy, P. Monks, R. Leigh, Air quality affected by trees in real street canyons: the case of Marylebone neighbourhood in central London, *Urban for, Urban Green* 22 (2017) 41–53, <https://doi.org/10.1016/j.ufug.2017.01.009>.
- [18] J. Liu, Z. Cao, S. Zou, H. Liu, X. Hai, S. Wang, J. Duan, B. Xi, G. Yan, S. Zhang, Z. Jia, An investigation of the leaf retention capacity, efficiency and mechanism for atmospheric particulate matter of five greening tree species in Beijing, China, *Sci. Total Environ.* 616–617 (2018) 417–426, <https://doi.org/10.1016/j.scitotenv.2017.10.314>.
- [19] A. Wania, M. Bruse, N. Blond, C. Weber, Analysing the influence of different street vegetation on traffic-induced particle dispersion using microscale simulations, *J. Environ. Manag.* 94 (2012) 91–101, <https://doi.org/10.1016/j.jenvman.2011.06.036>.
- [20] A.F. Speak, J.J. Rothwell, S.J. Lindley, C.L. Smith, Urban particulate pollution reduction by four species of green roof vegetation in a UK city, *Atmos. Environ.* 61 (2012) 283–293, <https://doi.org/10.1016/j.atmosenv.2012.07.043>.
- [21] A. Sharma, P. Conry, H.J.S. Fernando, A.F. Hamlet, J.J. Hellmann, F. Chen, Green and cool roofs to mitigate urban heat island effects in the Chicago metropolitan area: evaluation with a regional climate model Green and cool roofs to mitigate urban heat island effects in the Chicago metropolitan area: evaluation with a regional, *Environ. Res. Lett.* 11 (2016) 64004.
- [22] K. Dzierżanowski, R. Popek, H. Gawrońska, A. Sæbø, S.W. Gawroński, Deposition of particulate matter of different size fractions on leaf surfaces and in waxes of urban forest species, *Int. J. Phytoremediation.* 13 (2011) 1037–1046, <https://doi.org/10.1080/15226514.2011.552929>.
- [23] M. Viecco, S. Vera, H. Jorquerá, W. Bustamante, J. Gironás, C. Dobbs, E. Leiva, Potential of particle matter dry deposition on green roofs and living walls vegetation for mitigating urban atmospheric pollution in semiarid climates, *Sustainability* 10 (2018) 2431, <https://doi.org/10.3390/su10072431>.
- [24] A. Sæbø, R. Popek, H. Nawrot, H.M. Hanslin, H. Gawronski, S.W. Gawronski, Plant species differences in particulate matter accumulation on leaf surfaces, *Sci. Total Environ.* 427–428 (2012) 347–354, <https://doi.org/10.1016/j.scitotenv.2012.03.084>.
- [25] L. Chen, C. Liu, R. Zou, M. Yang, Z. Zhang, Experimental examination of effectiveness of vegetation as bio-filter of particulate matters in the urban environment, *Environ. Pollut.* 208 (2015) 198–208, <https://doi.org/10.1016/j.envpol.2015.09.006>.
- [26] J. Santiago, R. Buccolieri, E. Rivas, H. Calvete-sogo, B. Sanchez, A. Martílli, R. Alonso, D. Elustondo, J.M. Santamaría, F. Martín, CFD modelling of vegetation barrier effects on the reduction of traffic-related pollutant concentration in an avenue of Pamplona, Spain, *Sustain. Cities Soc.* 48 (2019) 101559, <https://doi.org/10.1016/j.scs.2019.101559>.
- [27] A.B. Besir, E. Cuce, Green roofs and facades: a comprehensive review, *Renew. Sustain. Energy Rev.* 82 (2018) 915–939, <https://doi.org/10.1016/j.rser.2017.09.106>.
- [28] A.F. Speak, J.J. Rothwell, S.J. Lindley, C.L. Smith, Urban particulate pollution reduction by four species of green roof vegetation in a UK city, *Atmos. Environ.* 61 (2012) 283–293, <https://doi.org/10.1016/j.atmosenv.2012.07.043>.
- [29] Sergio Vera, Margareth Viecco, Héctor Jorquerá, Effects of biodiversity in green roofs and walls on the capture of fine particulate matter, *Urban Forestry & Urban Greening* 63 (2021) 127229, <https://doi.org/10.1016/j.ufug.2021.127229>. ISSN 1618-8667.
- [30] L. Malys, M. Musy, C. Inard, A hydrothermal model to assess the impact of green walls on urban microclimate and building energy consumption, *Build. Environ.* 73 (2014) 187–197, <https://doi.org/10.1016/j.buildenv.2013.12.012>.

[31] M. Ottel, H.D. van Bohemen, A.L.A. Fraaij, Quantifying the deposition of particulate matter on climber vegetation on living walls, *Ecol. Eng.* 36 (2010) 154–162, <https://doi.org/10.1016/j.ecoleng.2009.02.007>.

[32] P. Conry, A. Sharma, M.J. Potosnak, L.S. Leo, E. Bensman, J.J. Hellmann, H.J. S. Fernando, Chicago's heat island and climate change: bridging the scales via dynamical downscaling, *J. Appl. Meteorol. Climatol.* 54 (2015) 1430–1448, <https://doi.org/10.1175/JAMC-D-14-0241.1>.

[33] Z. Tong, R.W. Baldauf, V. Isakov, P. Deshmukh, K. Max Zhang, Roadside vegetation barrier designs to mitigate near-road air pollution impacts, *Sci. Total Environ.* 541 (2016) 920–927, <https://doi.org/10.1016/j.scitotenv.2015.09.067>.

[34] J. Yang, H. Wang, B. Xie, Accumulation of Particulate Matter on Leaves of Nine Urban Greening Plant Species with Different Micromorphological Structures in Beijing, 28, 2015, p. 13198, <https://doi.org/10.13198/j.issn.1001-6929.2015.03.08>.

[35] F.J. Escobedo, J.E. Wagner, D.J. Nowak, C.L. De la Maza, M. Rodriguez, D.E. Crane, Analyzing the cost effectiveness of Santiago, Chile's policy of using urban forests to improve air quality, *J. Environ. Manag.* 86 (2008) 148–157, <https://doi.org/10.1016/j.jenvman.2006.11.029>.

[36] B.A. Currie, B. Bass, Estimates of air pollution mitigation with green plants and green roofs using the UFORE model, *Urban Ecosyst.* 11 (2008) 409–422, <https://doi.org/10.1007/s11252-008-0054-y>.

[37] A.P.R. Jeanjean, P.S. Monks, R.J. Leigh, Modelling the effectiveness of urban trees and grass on PM2.5 reduction via dispersion and deposition at a city scale, *Atmos. Environ.* 147 (2016) 1–10, <https://doi.org/10.1016/j.atmosenv.2016.09.033>.

[38] S. Vranckx, P. Vos, B. Maiheu, S. Janssen, Impact of trees on pollutant dispersion in street canyons: a numerical study of the annual average effects in Antwerp, Belgium, *Sci. Total Environ.* 532 (2015) 474–483, <https://doi.org/10.1016/j.scitotenv.2015.06.032>.

[39] R. Buccolieri, S.M. Salim, L.S. Leo, S. Di Sabatino, A. Chan, P. Ielpo, G. de Gennaro, C. Gromke, Analysis of local scale tree-atmosphere interaction on pollutant concentration in idealized street canyons and application to a real urban junction, *Atmos. Environ.* 45 (2011) 1702–1713, <https://doi.org/10.1016/j.atmosenv.2010.12.058>.

[40] C. Gromke, R. Buccolieri, S. Di Sabatino, B. Ruck, Dispersion study in a street canyon with tree planting by means of wind tunnel and numerical investigations - evaluation of CFD data with experimental data, *Atmos. Environ.* 42 (2008) 8640–8650, <https://doi.org/10.1016/j.atmosenv.2008.08.019>.

[41] J.J. Baik, K.H. Kwak, S.B. Park, Y.H. Ryu, Effects of building roof greening on air quality in street canyons, *Atmos. Environ.* 61 (2012) 48–55, <https://doi.org/10.1016/j.atmosenv.2012.06.076>.

[42] P.E.J. Vos, B. Maiheu, J. Vankerkom, S. Janssen, Improving local air quality in cities: to tree or not to tree? *Environ. Pollut.* 183 (2013) 113–122, <https://doi.org/10.1016/j.envpol.2012.10.021>.

[43] F. Bottalico, G. Chirici, F. Giannetti, A. De Marco, S. Nocentini, E. Paoletti, F. Salbitano, G. Sanesi, C. Serenelli, D. Travaglini, Air pollution removal by green infrastructures and urban forests in the city of florence, *Agric. Agric. Sci. Procedia* 8 (2016) 243–251, <https://doi.org/10.1016/j.aaspro.2016.02.099>.

[44] H. Qin, B. Hong, R. Jiang, Are green walls better options than green roofs for mitigating PM10 pollution? CFD simulations in urban street canyons, *Sustainability* 10 (2018) 2833.

[45] M. Bruce, Envi-met, 2008. <https://www.envi-met.com/about-us/>.

[46] S. Tsoka, A. Tsikaloudaki, T. Theodosiou, Analyzing the ENVI-met microclimate model's performance and assessing cool materials and urban vegetation applications-a review, *Sustain. Cities Soc.* 43 (2018), <https://doi.org/10.1016/j.scs.2018.08.009>.

[47] V.P. López-Cabeza, C. Galán-Marín, C. Rivera-Gómez, J. Roa-Fernández, Courtyard microclimate ENVI-met outputs deviation from the experimental data, *Build. Environ.* 144 (2018) 129–141.

[48] D.H.S. Duarte, P. Shinzato, S. Gusson, C.A. Alves, Urban Climate the impact of vegetation on urban microclimate to counterbalance built density in a subtropical changing climate, *Urban Clim.* 14 (2015) 224–239, <https://doi.org/10.1016/j.uclim.2015.09.006>.

[49] R.C. Muñoz, A.A. Undurraga, Daytime mixed layer over the Santiago Basin: description of two years of observations with a lidar ceilometer, *J. Appl. Meteorol. Climatol.* 49 (2010) 1728–1741, <https://doi.org/10.1175/2010JAMC2347.1>.

[50] B. Paas, C. Schneider, A comparison of model performance between ENVI-met and Austral2000 for particulate matter, *Atmos. Environ.* 145 (2016) 392–404, <https://doi.org/10.1016/j.atmosenv.2016.09.031>.

[51] M. Kottek, J. Grieser, C. Beck, B. Rudolf, F. Rubel, World map of the Köppen-Geiger climate classification updated, *Meteorol. Z.* 15 (2006) 259–263, <https://doi.org/10.1127/0941-2948/2006/0130>.

[52] H. Jorquera, Ambient particulate matter in Santiago, Chile: 1989–2018: a tale of two size fractions, *J. Environ. Manag.* 258 (2020), 110035, <https://doi.org/10.1016/j.jenvman.2019.110035>.

[53] A.M. Villalobos, F. Barraza, H. Jorquera, J.J. Schauer, Chemical speciation and source apportionment of fine particulate matter in Santiago, Chile, 2013, *Sci. Total Environ.* 512–513 (2015) 133–142, <https://doi.org/10.1016/j.scitotenv.2015.01.006>.

[54] H. Jorquera, W. Palma, J. Tapia, An intervention analysis of air quality data at Santiago, Chile, *Atmos. Environ. Times* 34 (2000) 4073–4084.

[55] MMA, Sistema de Información Nacional de Calidad del Aire. <http://sinca.mma.gob.cl/>, 2017. (Accessed 1 July 2017).

[56] R.A. Johnson, Probabilidad y estadística para ingenieros, Pearson Educación, 2012.

[57] G. Rushingabigwi, P. Nsengiyumva, L. Sibomana, C. Twizere, W. Kalisa, Analysis of the atmospheric dust in Africa: the breathable dust's fine particulate matter PM2.5 in correlation with carbon monoxide, *Atmos. Environ.* 224 (2020) 117319.

[58] W. Yang, H. Chen, J. Wu, W. Wang, J. Zheng, D. Chen, J. Li, X. Tang, Z. Wang, L. Zhu, Characteristics of the source apportionment of primary and secondary inorganic PM2.5 in the Pearl River Delta region during 2015 by numerical modeling, *Environ. Pollut.* 267 (2020) 115418.

[59] Y.-J. Choi, P. Hyde, H.J.S. Fernando, Modeling of episodic particulate matter events using a 3-D air quality model with fine grid: applications to a pair of cities in the US/Mexico border, *Atmos. Environ.* 40 (2006) 5181–5201.

[60] Y.-J. Choi, H.J.S. Fernando, Implementation of a windblown dust parameterization into MODELS-3/CMAQ: application to episodic PM events in the US/Mexico border, *Atmos. Environ.* 42 (2008) 6039–6046.

[61] P.E. Saide, G.R. Carmichael, S.N. Spak, L. Gallardo, A.E. Osses, M.A. Mena-Carrasco, M. Pagowski, Forecasting urban PM10 and PM2.5 pollution episodes in very stable nocturnal conditions and complex terrain using WRF-Chem CO tracer model, *Atmos. Environ.* 45 (2011) 2769–2780.

[62] DICTUC, Actualización de perfiles de flujos del modelo MODEM para el Gran Santiago y regiones, 2016. <http://www.sectra.gob.cl/biblioteca/detalle1.asp?mf=3377>.

[63] J.M. Perez-Blanco, Conventional & Green Roof Albedo Measurement and Analysis for Roof-Mounted Photovoltaic Applications, Pennsylvania State University., 2010.

[64] C.A. Belis, D. Pernigotti, G. Pirovano, O. Favez, J.L. Jaffrezo, J. Kuenen, H.D. Van Der Gon, M. Reizer, V. Riffault, L.Y. Alleman, M. Almeida, F. Amato, A. Anygal, G. Argyropoulos, S. Bande, I. Beslic, J. Besombes, M.C. Bove, P. Brotto, G. Calori, D. Cesari, C. Colombi, D. Contini, G. De Gennaro, A. Di Gilio, E. Diapouli, I. El Haddad, H. Elbern, K. Eleftheriadis, J. Ferreira, M.G. Vivanco, S. Gilardoni, B. Golly, S. Hellebust, P.K. Hopke, Y. Izadmanesh, H. Jorquera, K. Krajsek, R. Kranenburg, P. Lazzeri, F. Lenartz, F. Lucarelli, K. Maciejewska, A. Manders, M. Manouskas, M. Masiol, M. Mircea, D. Moobroek, S. Nava, D. Oliveira, M. Paglione, M. Pandolfi, M. Perrone, E. Petralia, A. Pietrodangelo, S. Pillon, P. Pokorna, P. Prati, D. Salameh, C. Samara, L. Samek, D. Saraga, S. Sauvage, M. Schaap, F. Scotto, K. Segu, G. Siour, R. Tauler, G. Valli, R. Vecchi, E. Venturini, M. Vestenius, A. Waked, E. Yubero, Evaluation of receptor and chemical transport models for PM10 source apportionment, *Atmos. Environ. X* (2019) 100053, <https://doi.org/10.1016/j.aeaoa.2019.100053>.